EGU2020: Sharing Geoscience Online, 4–8 May 2020

Multi-temporal mapping of pantropical post-loss land cover using dense earth-observation time series and global pre-existing maps

Alejandro Coca-Castro[1,2], Louis Reymondin[2], and Mark Mulligan[1]

1 Department of Geography, King's College London, UK

2 Decision and Policy Analysis Research Area, International Center for Tropical Agriculture, Colombia

KING'S College LONDON

CIAT International Center for Tropical Agriculture Since 1967 Science to cultivate change

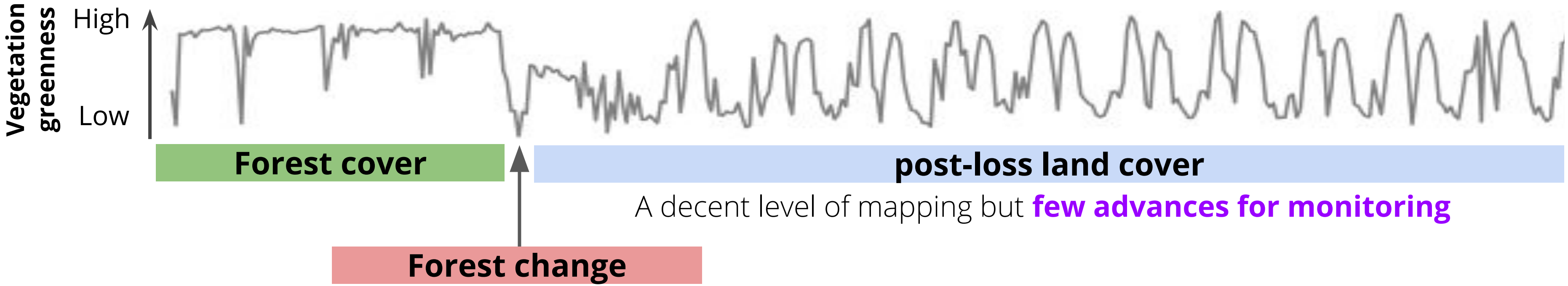

Why land cover information over deforested areas (so-called post-loss LC) ?

15 LIFE ON LAND

Supports national plans of payments for forest conservation schemes (SGD 15) and climate mitigation (SDG 13)

Contributes in modelling policy and planning scenarios for (agro)ecosystems management (zero-deforestation supply chains) and conservation (deforestation pathways) in tropics

13 CLIMATE ACTION

Aims and objectives

To predict post-loss LC over deforested areas as detected by Terra-i, an early warning system of pantropical forest change providing alerts every 16-days from 2004 to present at spatial resolution of 250-m.

- **O1:** Assessing a supervised deep neural network model suited to extract spatio-temporal patterns from dense earth observation time series data according to different labelled datasets representing different number of LC classes and complexity.
- **O2:** Comparing results of the best suited labelled datasets for the model against a regional-tuned LC dataset for the period 2001-2017.

A supervised deep neural network learning model

The Multitemporal Land Cover Classification (MTLCC) Network

A General Recurrent Unit (GRU) cell

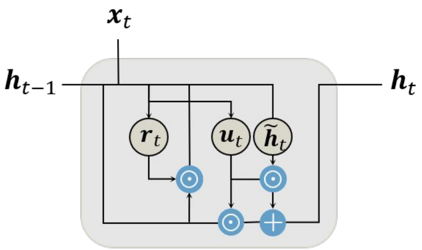

where:

input (x_t)

States: previous (h_{t-1}) and current (h_t)

update gate (u_t)

reset gate (r_t)

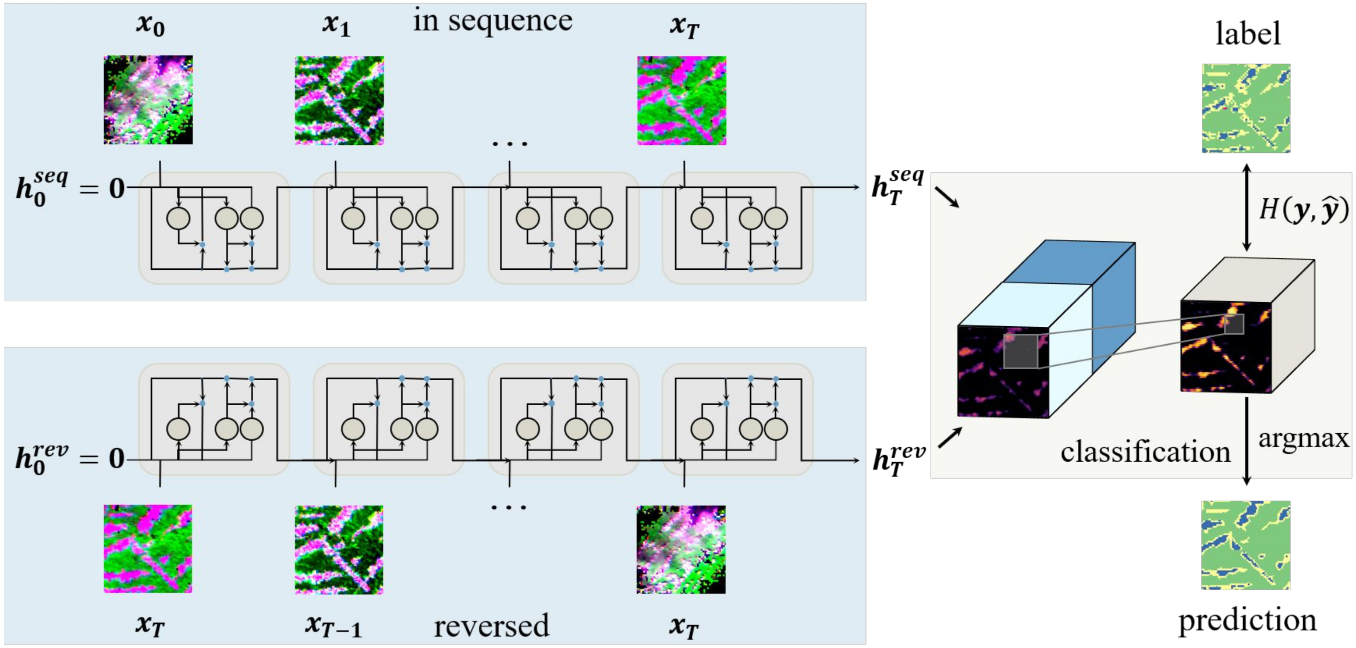

Fig 1. Adapted scheme of the MTLCC model assessed within this work. Tunable hyper-parameters are the number of layers l, number of recurrent cells r and the sizes of the convolutional kernel $krnn$ and the classification kernel $kclass$. Original source: **Rußwurm and Korner (2018)**.

Model inputs

Dense earth-observation time series (x)

Surface reflectance:

- MOD09Q1 (v6) TERRA , 8-d, 250-m, 2 bands (**red, NIR**)
- MOD09A1 (v6) TERRA , 8-d, 500-m, 5 bands (**blue, gren, SWIR1, SWIR2, SWIR3**) > downscaled to 250-m (bilinear interpolation)

Time information:

Day of the year (**DOY**) extracted from satellite images

Why MODIS?

- Long-term records (2000 onwards), 46 observations by year
- Match with the spatial resolution of the reference deforestation product, Terra-i (250-m)

Model inputs

Labels ('ground-truth') (y)

ID	Short name	Scheme	Number of classes (excl. no data)	Source (and version)	Resolution (m)	Temporal coverage (annual)
1	MODIS IGBP	IGBP	17	MCD12Q1 v6	500	2001-2017
2	MODIS FAO-LCCS1	FAO-LCCS	16	MCD12Q1 v6	500	2001-2017
3	MODIS FAO-LCCS2	FAO-LCCS	11	MCD12Q1 v6	500	2001-2017
4	ESA FAO-LCCS	FAO-LCCS	37	ESA-LC-CCI v2.0.7	300	2001-2015
5	CGLS-LC100 FAO-LCCS	FAO-LCCS	22	CGLS-LC100 v2	100	2015
6	MapBiomas Custom	Custom	9	MapBiomas Amazonia v1	30	2001-2017

5 datasets derived from a common year (2015) of 5 pre-existing global LC products **(IDs 1-5 in the table)** with a native spatial resolution ranging from 100 m to 500 m.

Remaining datasets called 'hybrid' (4 in total) were generated by exploiting temporal **(ID 3)** spatial **(ID 5)**, and semantic **(ID 3 to 5)** properties of the pre-existing LC products

→ **Only for comparison (O2)**

Model inputs

Description of the hybrid datasets (4 in total) derived from global LC products

Semantic/Spatial (1)

O8* dataset refers to the integration of three LC global products (i) MODIS FAO-LCCS2 (N=11); (ii) ESA FAO-LCCS (N=37) and (iii) CGLS-LC100 FAO-LCCS (N=22).

Map legends were harmonized to eight general LC classes.

Reclassified maps were overlapped.

Pixels which do not overlap in all three datasets were classified as *NoData.*

Spatial (1)

C9* dataset exploits the subpixel information offered by the CGLS-LC100 dataset.

It reflects small-scale disturbances which are mislead in the resampled CGLS-LC100 dataset from 100-m to 250-m.

Based on the proportion of *Closed forest pixels* computed at the extent of MODIS 250-m.

Replaced a given fraction of *Closed forest* with the predominant non-closed forest class per pixel.

Temporal (2)

2001-2015 MODIS IGBP (M17*), 2001-2015 MODIS FAO-LCCS2 (M11*) datasets exploit pixels with LC types that had not changed from a considerable length of time.

This particular procedure was only applied for two out of three LC schemes in the MODIS Land Cover Type product (2001-2018)

Only the stable pixels from 2001 to 2015, which end year matches with the year of analysis of this work, were considered.

Workflow

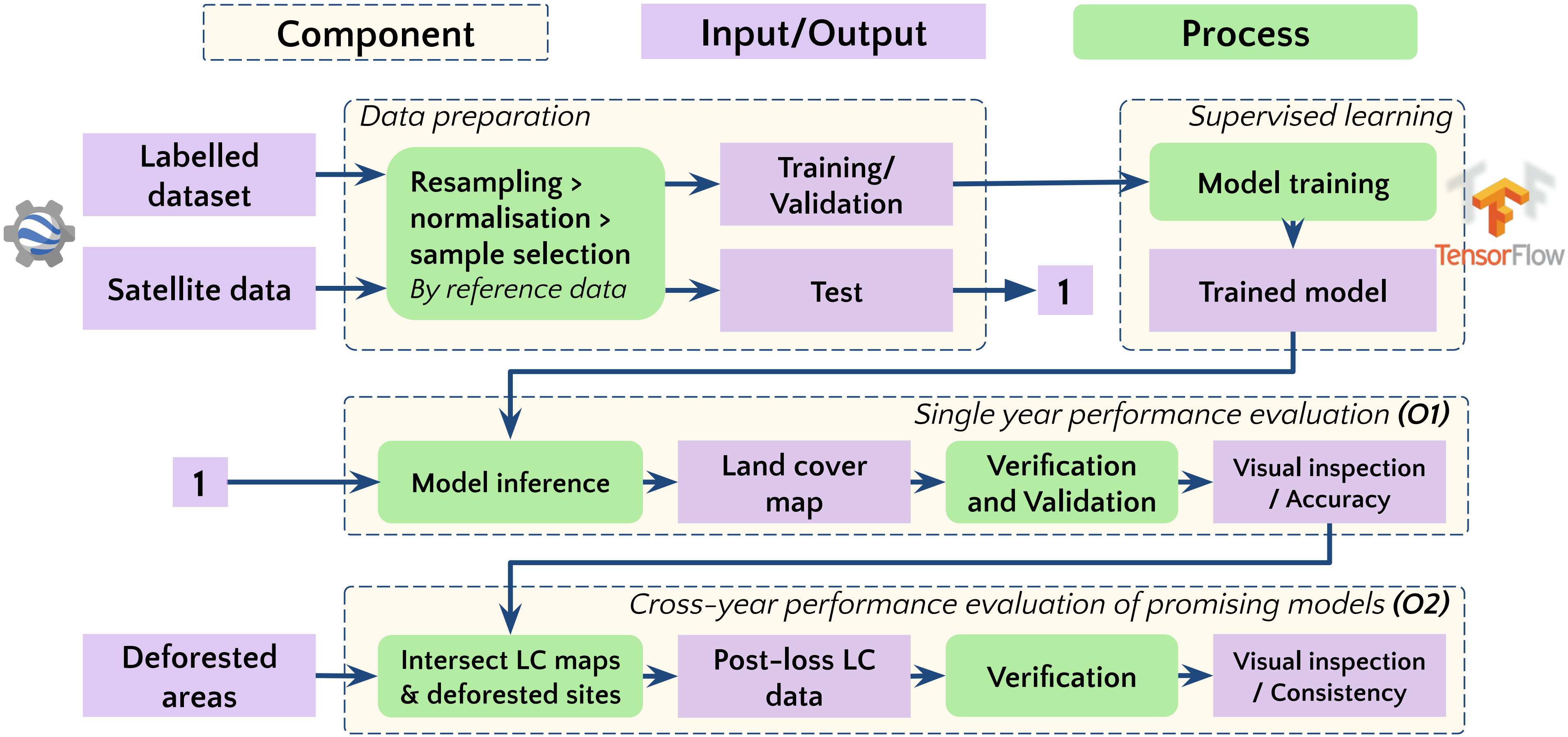

Component
Input/Output
Process
Data preparation
Supervised learning
Labelled dataset
Satellite data
Resampling > normalisation > sample selection
By reference data
Training/ Validation
Test
1
Model training
Trained model
TensorFlow
Single year performance evaluation (O1)
1
Model inference
Land cover map
Verification and Validation
Visual inspection / Accuracy
Cross-year performance evaluation of promising models (O2)
Deforested areas
Intersect LC maps & deforested sites
Post-loss LC data
Verification
Visual inspection / Consistency

Software and Implementation

Satellite data and LC products acquired from Google Earth Engine

Configuration of the MTLCC model > ‘trial and error’ (Coca-Castro et al., 2019)

- Batch size of {32}
- Layers - l: {1}
- Recurrent cells (GRU) - r: {64}
- Trained over **30 epochs** on data of **2015**

Models’ performance assessed over validation split by year
Metrics: traditional metrics (e.g. overall accuracy, recall, precision, f-score), and others with land change and remote sensing research foci (e.g. kappa, disagreement metrics)

- Modified source code from Rußwurm and Körner (2018)
- Models built with Tensorflow v.1.7.0.
- GPU processing (Tesla M60, 16GB DDR5)

The study area: The Amazon as defined by [RAISG]

Visualisation of the study area and a labelled dataset (MODIS IGBP - 17 LC classes) for 2015

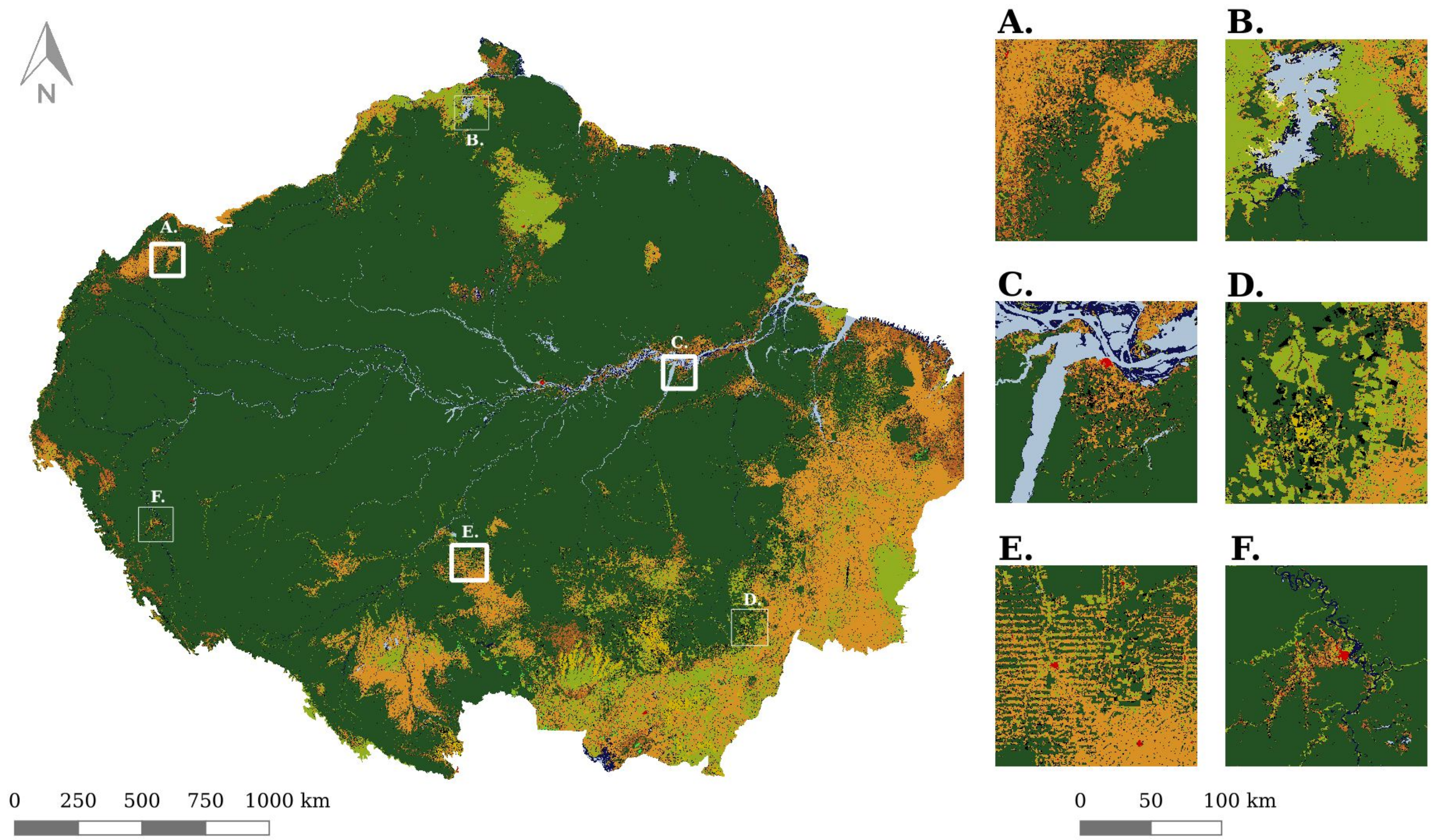

Data preparation (partition) and distribution

Data partition (train, test and eval - 4:1:1)

Block-wise spatial design yielding:

177 train blocks
45 validation blocks
45 test blocks

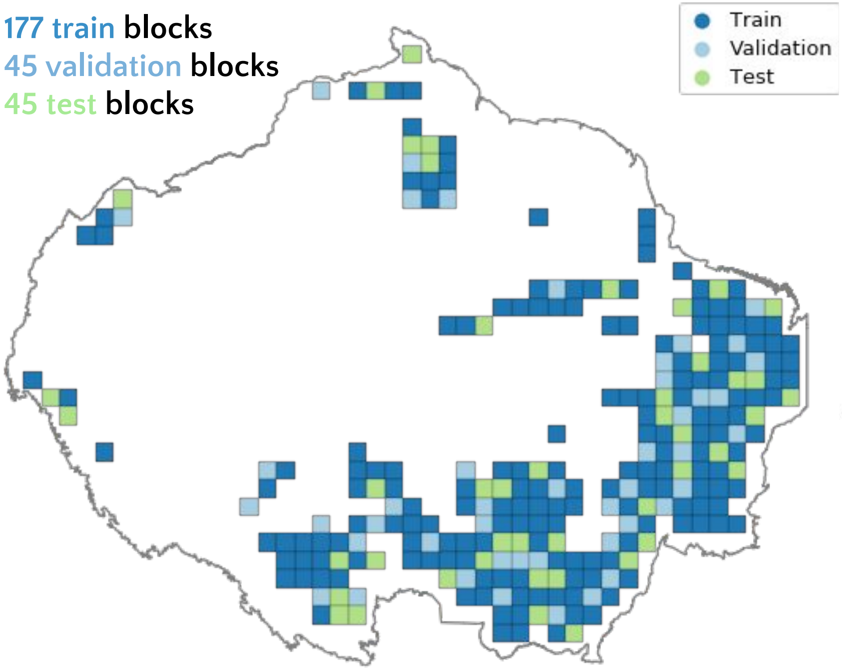

Block size = 384 px x 384 px
Model trained using 24 px x 24 px

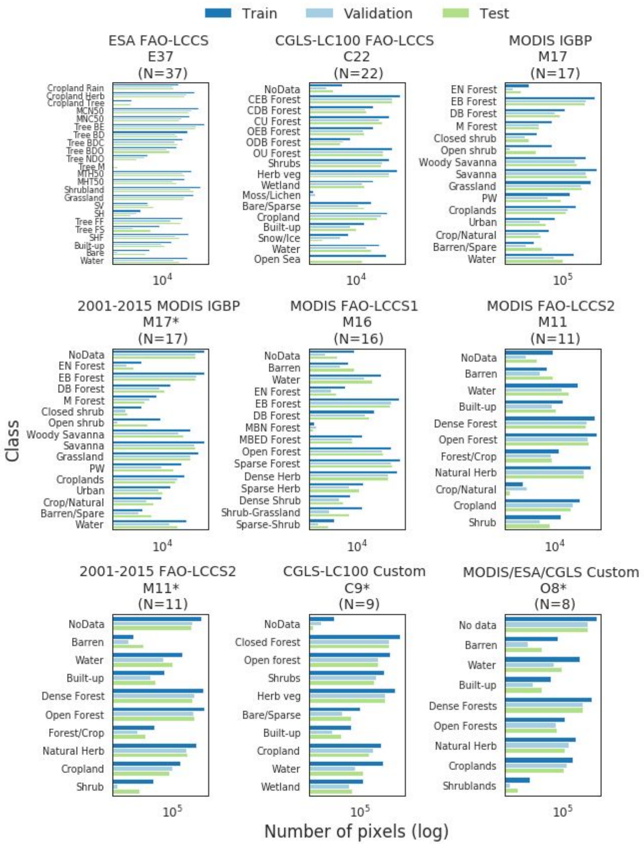

MODIS satellite observations from a single year, 2015, were used to create pairs (input & labels) to train and evaluate the performance of the model.

Why?
This is a common year between all pre-existing LC products used

Results

Single year (2015) performance evaluation - Quantitative

Table 1. Averaged values (± one standard deviation) of pixel-wise accuracy metrics over five folds of the MTLCC network model trained with target datasets.

Labelled dataset	Overall accuracy (OA) (%)	Quantity Disagreement (%)	Allocation Disagreement (%)	Kappa (κ)	
ESA FAO-LCCS (E37)	66.46 ± 0.26	13.61 ± 1.69	19.92 ± 1.87	0.57 ± 0.0	
CGLS-LC100 FAO-LCCS (C22)	63.37 ± 1.68	7.38 ± 2.26	29.24 ± 0.89	0.51 ± 0.03	
MODIS IGBP (M17)	79.96 ± 0.89	7.61 ± 2.15	12.43 ± 1.53	0.72 ± 0.01	
2001-2015 MODIS IGBP (M17*)	86.36 ± 0.64	5.34 ± 0.39	8.31 ± 0.64	0.81 ± 0.01	*
MODIS FAO-LCCS1 (M16)	81.24 ± 0.59	7.23 ± 3.21	11.52 ± 2.64	0.74 ± 0.01	
MODIS FAO-LCCS2 (M11)	84.92 ± 0.85	2.89 ± 1.42	12.19 ± 1.06	0.77 ± 0.01	
2001-2015 MODIS FAO-LCCS2 (M11*)	89.17 ± 1.00	4.81 ± 1.56	6.02 ± 0.85	**0.83 ± 0.02**	*
CGLS-LC100 Custom (C9*)	69.48 ± 2.01	5.58 ± 1.06	24.94 ± 2.09	0.56 ± 0.03	*
MODIS/ESA/CGLS Custom (O8*)	**92.35 ± 0.48**	**3.68 ± 1.03**	**3.97 ± 1.44**	0.74 ± 0.01	*

Models trained using hybrid datasets (*) performed better than the original.

The hybrid dataset MODIS/ESA/CGLS (O8*) returned the highest overall accuracy, 92.35±0.48 over the 45 test tiles. Other hybrid datasets related to multi-year stable pixels from MODIS dataset, 2001-2015 MODIS IGBP (M17*) and 2001-2015 MODIS FAO-LCCS2 (M11*) provided a notable gain in OA compared to the original datasets.

The spatial-based hybrid C9* dataset yields good results against C22.

Results

Single year (2015) performance evaluation - Qualitative top 3 datasets (O8*, M11*, C9*)

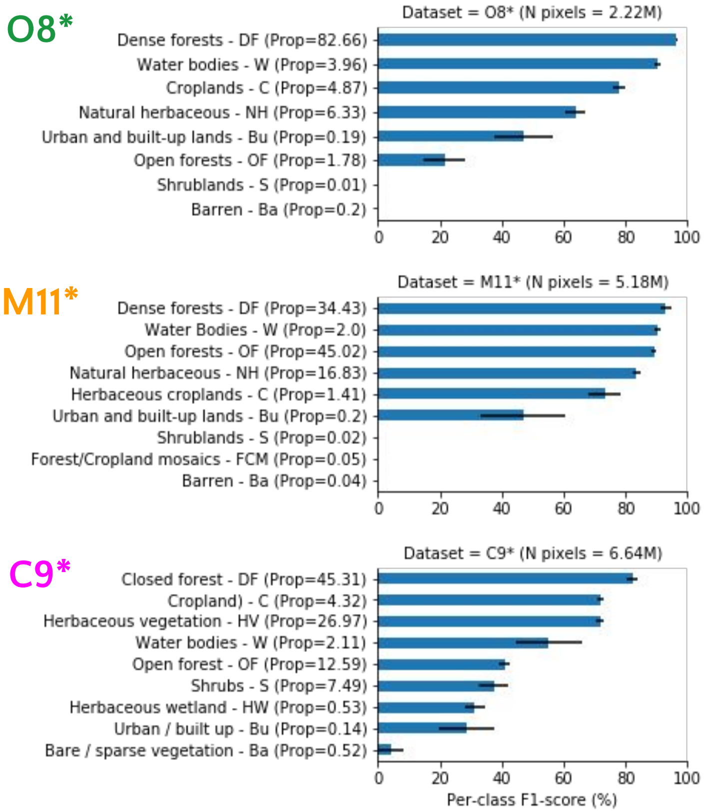

Fig 1. Per-class F1-score of top 3 datasets

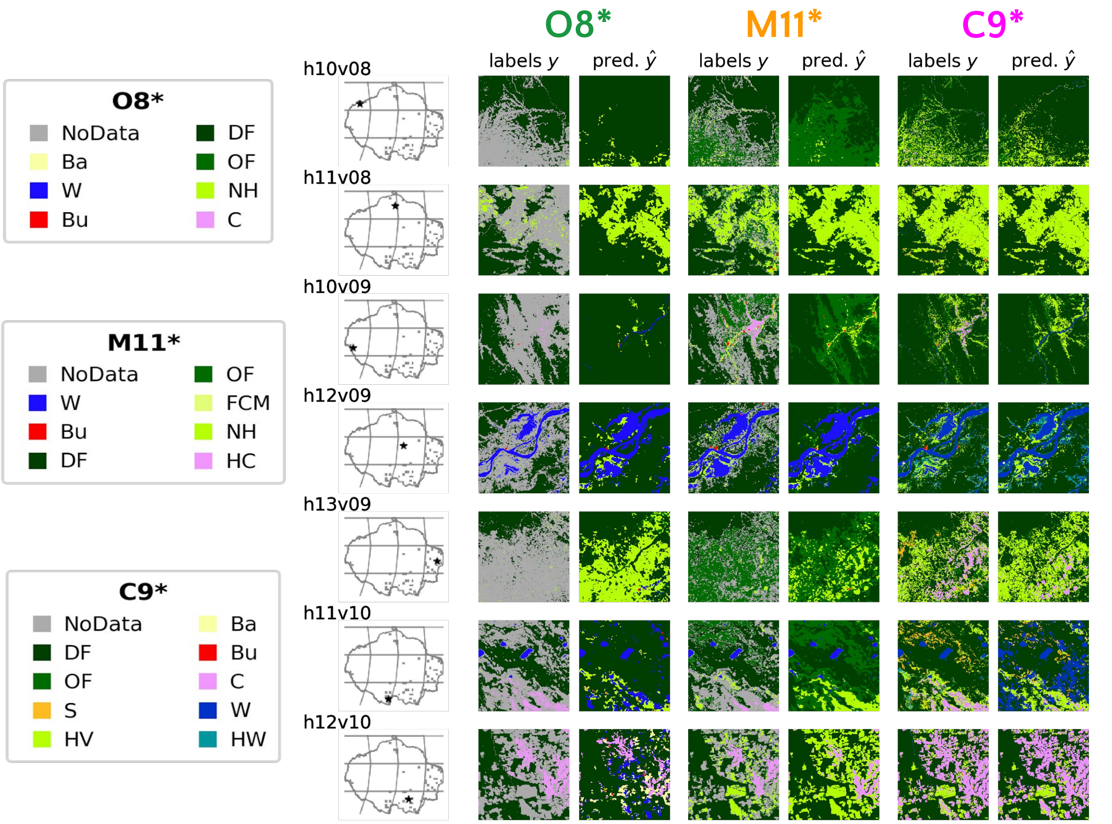

Fig 2. Labels (ground-truth) and predictions per dataset

Results

Cross-year evaluation across 7 test tiles distributed over MODIS scenes in the AOI

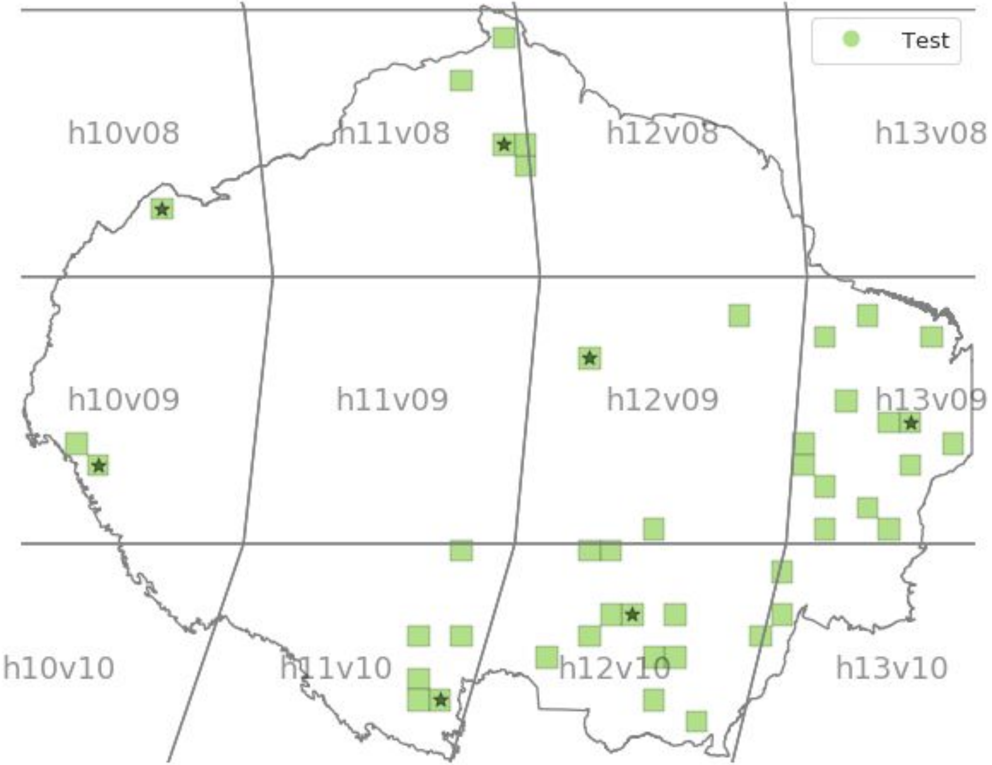

Fig 1. Distribution of the sampled tiles (★) for the cross-year evaluation.

This section presents a visual inspection of the spatio-temporal consistency of the LC predictions by the trained models using **C9*** and **M11*** datasets across 17 years of MODIS imagery.

Only **annual LC data** was observed in **a single deforestation year**, in this case the peak year of Terra-i's deforestation data from 2004 to 2010, per sampled tile.

The analysis over **three out of seven sampled** tiles, which shows contrast in clearing sizes and locations across the study area, is presented as follows.

Results

Tile h12v10: large area clearings in the eastern Amazon

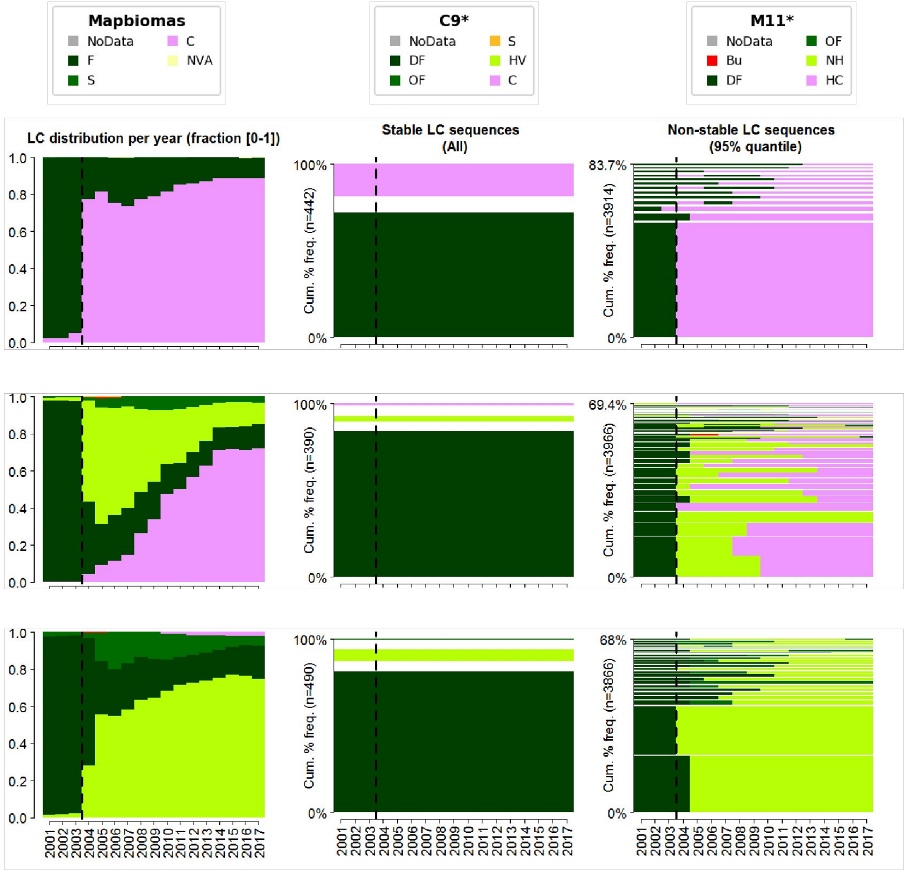

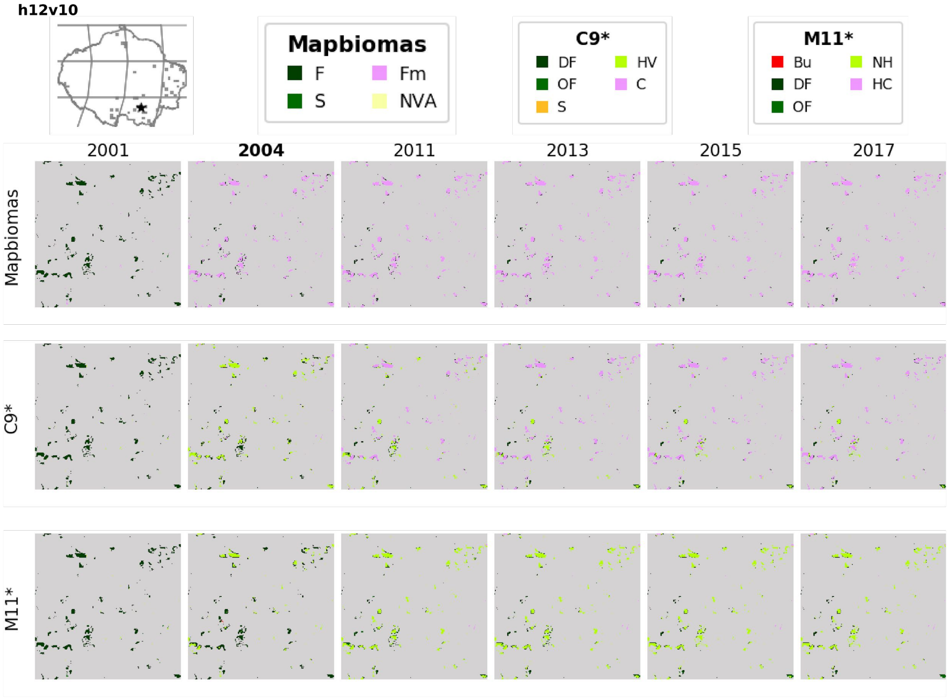

Fig 1. Subset of 2001–2017 annual LC extracted from the MapBiomas dataset and predictions by the MTLCC network trained using **C9*** and **M11*** datasets. The peak deforestation year is highlighted in **bold**.

Results

Tile h10v08: small area clearings in the northwest Amazon

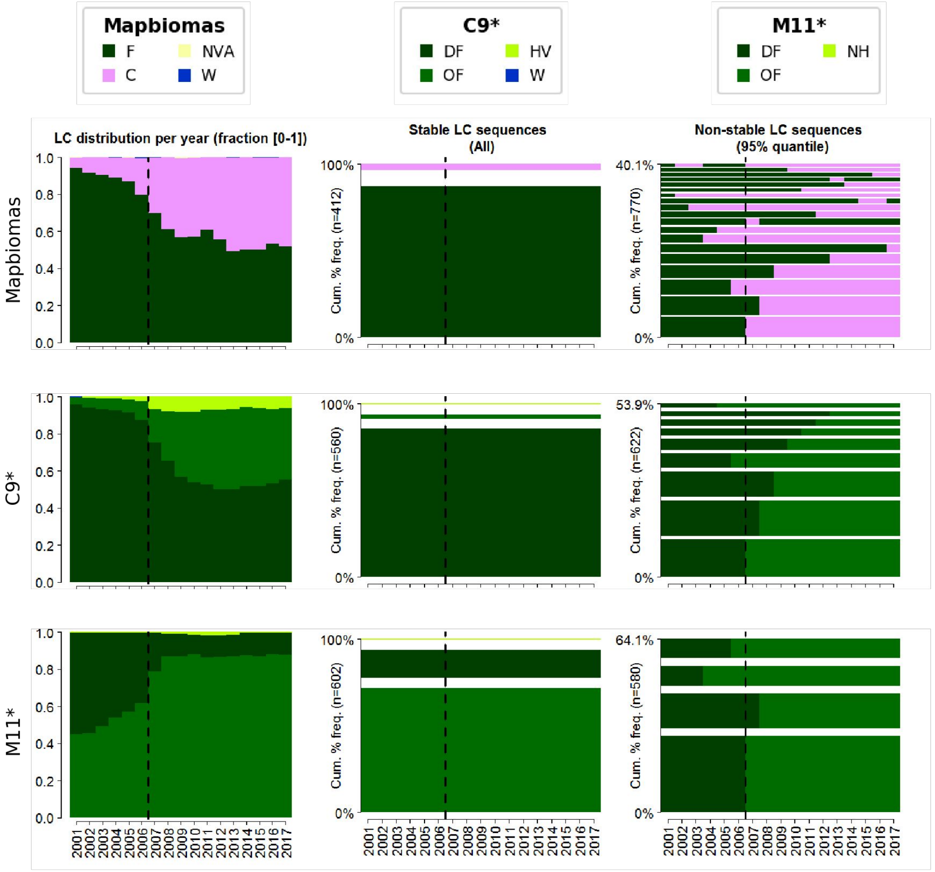

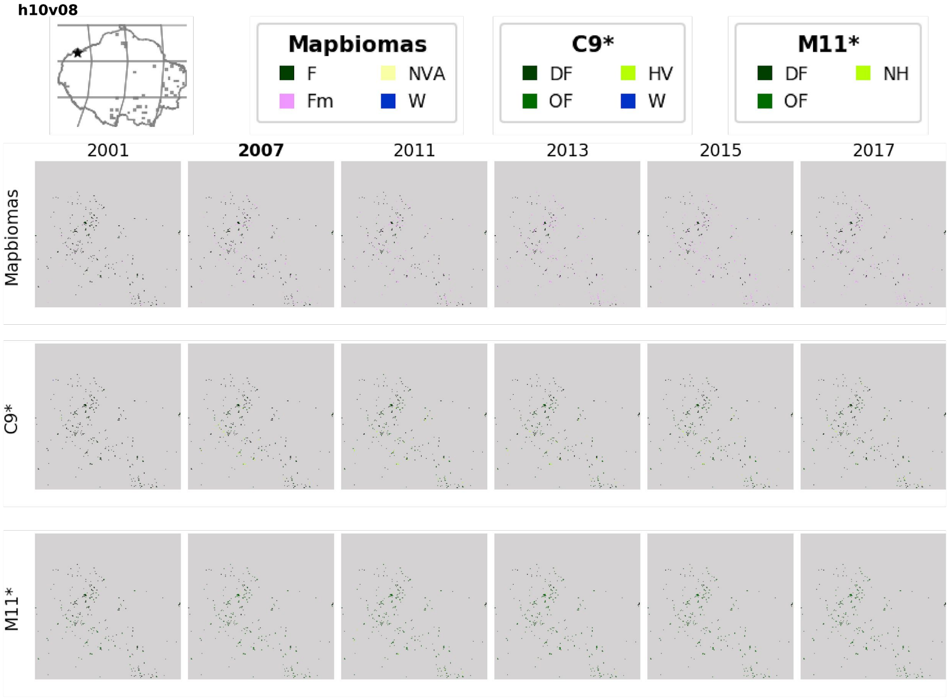

Fig 1. Subset of 2001-2017 annual LC extracted from the MapBiomas dataset and predictions by the MTLCC network trained using **C9*** and **M11*** datasets. The peak deforestation year is highlighted in **bold**.

Results

Tile h10v09: small area clearings in the western Amazon

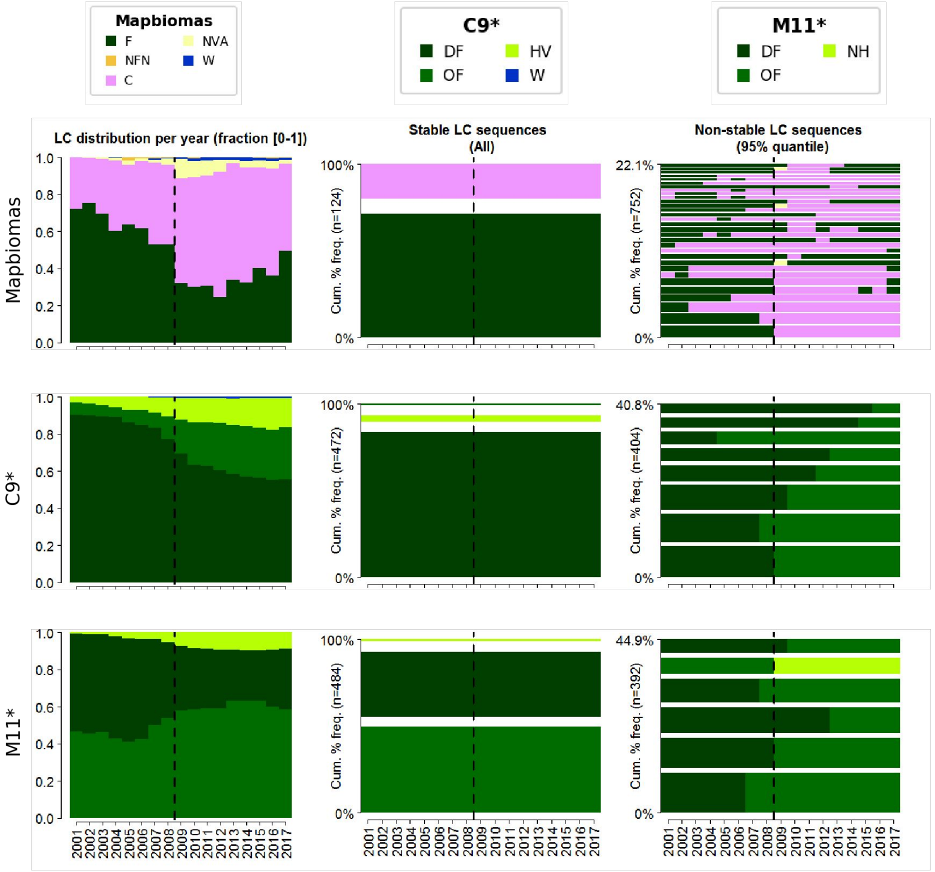

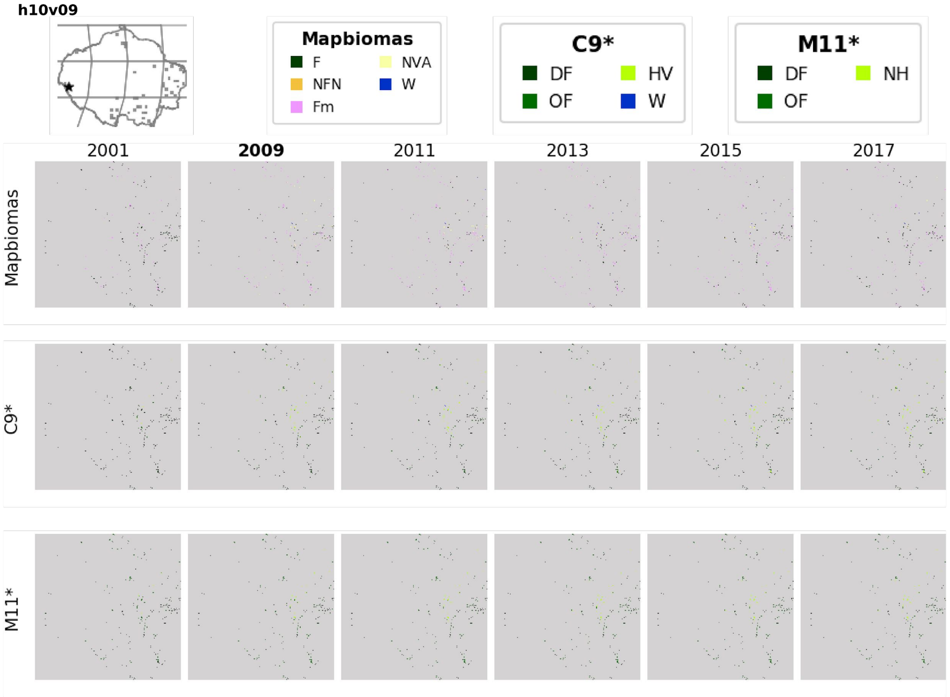

Fig 1. Subset of 2001–2017 annual LC extracted from the MapBiomas dataset and predictions by the MTLCC network trained using C9* and M11* datasets. The peak deforestation year is highlighted in **bold**.

Conclusions

- The capability of the MTLCC model in predicting LC using dense earth-observation time series at a spatial resolution of 250-m, is influenced by characteristics of the training dataset (size, number of classes, labels noise).
- Hybrid datasets yielded better performance than original LC products.
- A visual inspection of the predictions corroborated the hybrid datasets **C9*** and **M11*** datasets as having a better generalization than the **O8*** hybrid dataset.
- The trained MTLCC models using the **C9*** and **M11*** datasets were spatially and temporally consistent in a tile with large-area disturbed sites but were unable to capture possible LC sequences in tiles with small-area disturbances.
- The MTLCC network trained with **C9*** provided coherent spatio-temporal predictions for the study of post-loss LC > partially explained by the level of detail provided by native spatial resolution of the C9* (100-m).
- **M11*** still offers a greater suitability for mapping post-loss LC change trajectories > noisy labels are reduced by using the temporal attributes of its original dataset.

Acknowledgements: The authors acknowledge Fundación CEIBA (funding), CIAT (hardware) and Marc Rußwurm (MTLCC model)